PNL-2265-3
UC-70

Quarterly Progress Report Research and Development Activities Waste Fixation Program July Through September 1977

J. L. McElroy

October 1978

Prepared for the U.S. Department of Energy
under Contract EY-76-C-06-1830

Pacific Northwest Laboratory
Operated for the U.S. Department of Energy
by Battelle Memorial Institute

PNL-2265-3

Battelle

PACIFIC NORTHWEST LABORATORY
operated by
BATTELLE
for the
UNITED STATES DEPARTMENT OF ENERGY
Under Contract EY-76-C-06-1830

Printed in the United States of America
Available from
National Technical Information Service
United States Department of Commerce
5285 Port Royal Road
Springfield, Virginia 22151

Price: Printed Copy $____*; Microfiche $3.00

*Pages	NTIS Selling Price
001-025	$4.00
026-050	$4.50
051-075	$5.25
076-100	$6.00
101-125	$6.50
126-150	$7.25
151-175	$8.00
176-200	$9.00
201-225	$9.25
226-250	$9.50
251-275	$10.75
276-300	$11.00

DISCLAIMER

PNL-2265-3
UC-70

QUARTERLY PROGRESS REPORT RESEARCH AND DEVELOPMENT ACTIVITIES WASTE FIXATION PROGRAM JULY THROUGH SEPTEMBER 1977

J. L. McElroy

October 1978

Prepared for
the U.S. Department of Energy
under Contract EY-76-C-06-1830

Pacific Northwest Laboratory
Richland, Washington 99352

SUMMARY

Through the Waste Fixation Program, the Pacific Northwest Laboratory is conducting research on the solidification of high-level radioactive waste. A major goal of this program is to develop reliable solidified waste forms and processes for their manufacture. This progress report describes the research and development activities of the past quarter:

- Over 25,500 lb of glass incorporating simulated defense waste was manufactured in a joule-heated ceramic melter this quarter. In one 86-hr period of continuous operation, 15,000 lb of glass was manufactured.
- The melting rate in the in-can melting process was found to be approximately proportional to the diameter of the canister, being 50, 70 and 90 kg/hr in canisters with 12-, 16-, and 20-in. diameters.
- We installed a new, highly instrumented, high-capacity effluent system that serves all of the calciners and melters in the engineering development laboratory.
- Preliminary leach tests of waste glass in salt brine at 250°C and 1000 psi yielded leach rates of between 2×10^{-4} and 7×10^{-4} g/cm^2-day -- about the same as other similarly tested materials such as granite, alumina, and LWR fuel pellets.
- A Pb-10Sn alloy continued to appear superior to plain lead as a metal matrix material for waste glass marbles, based upon an examination of the interfacial area after heat treatments.

PREVIOUS REPORTS

Previous reports in this series were BNWL-1699, -1741, -1761, -1788, -1809, -1826, -1841, -1871, -1893, -1908, -1932, -1949, -1994, -2070, -2242, -2243, -2264, and PNL-2265-1 and -2265-2.

CONTENTS

CONTENTS (Contd.)

FIGURES

TABLES

QUARTERLY PROGRESS REPORT
RESEARCH AND DEVELOPMENT ACTIVITIES
WASTE FIXATION PROGRAM
JULY THROUGH SEPTEMBER 1977

INTRODUCTION

The Waste Fixation Program (WFP) is conducted by the Pacific Northwest Laboratory (PNL), operated by Battelle Memorial Institute for the Department of Energy (DOE). Under this program, PNL is conducting research to convert high-level radioactive waste to stable, nondispersible forms. Canididate waste forms include silicate glasses and various crystalline and multibarrier waste forms. The WFP is designed to be a means through which the government and users of the technology can cooperate to effectively handle nuclear waste. Objectives of the comprehensive program include: the development and characterization of glass formulations; equipment and process development; and design, construction, and demonstration of full-scale process equipment. The following sections describe research and development activities in radioactive waste fixation for the past quarterly reporting period.

SECTION 1 - WASTE FIXATION PROCESS DEVELOPMENT

The purpose of this task is to develop processes and equipment for converting liquid high-level radioactive waste into a stable, relatively nondispersible form for storage and, ultimately, disposal. This purpose is generally being accomplished by the development of a two-step approach--calcination or concentration followed by melting to form a borosilicate glass.

JOULE-HEATED CERAMIC MELTER - C. C. Chapman and J. L. Buelt

The liquid-fed ceramic melter has been at melting temperature for seven months. This quarter's activities have involved simulated Hanford and Savannah River wastes and the direct conversion of liquid waste into glass. Using a simulated calcine waste from the Hanford radionuclide removal process, we filled four 9-ft canisters with 15,000 lb of melted glass over an 86-hr period. Other defense waste demonstrations have produced 6500 lb of glass. In liquid feeding tests, 730 ℓ of simulated liquid power reactor wastes have been successfully processed.

In addition, progress continues on the construction of a ceramic melter that is to be coupled to the full-scale spray calciner. The design process is also continuing on the laboratory-scale melter that will be used for small-scale testing purposes.

DEVELOPMENTAL SPRAY CALCINER - W. J. Mikols and L. S. Romero

Progress this quarter was marked by completion of seven developmental spray calciner runs. These runs successfully demonstrated the spray calciner's ability to dry several types of liquid feed solutions. Supercalcine, Rockwell Hanford Operations (RHO) defense waste calcine, and Savannah River Plant (SRP) defense waste calcine are among those produced. Other significant studies included: 1) a test with an external nozzle using steam atomization, and 2) continued measurements of ruthenium volatility.

IN-CAN MELTING - H. T. Blair

Melting rates of 50 kg/hr, 70 kg/hr, and 90 kg/hr were demonstrated this quarter in the full-scale in-can melter (ICM) for 12-in.-, 16-in.-, and 20-in.-dia cans, respectively. The full-scale ICM was modified to demonstrate bottom support of the can, location of the can completely within the furnace, and use of a new can configuration.

A melting rate of 70 kg/hr was sustained for over 5 hr in a 16-in.-dia can containing eight radial heat transfer fins. The can was suspended in the full-scale, multizone ICM furnace and maintained at 1070°C for the melting demonstration. Following this demonstration, the full-scale ICM system was modified to permit demonstration and evaluation of several significant new innovations in the ICM concept.

First, the load cells and the can suspension system were removed from the top of the furnace, and the load cells were located beneath the plug in the bottom of the furnace. This enabled the cans to be supported from the bottom and the load cells to be located where they would not be overheated. A new can configuration was introduced. These new cans are right-circular cylinders with flat tops and bottoms. There are no ears or bails on

them. The openings in the top centers of the cans are designed for twistlock closure. The cans are handled by engaging a plug, which has a bail on it, into the twistlock. The cans are 7 ft tall; when they are set on the plug in the bottom of the furnace the top of the can is 4 in. below the top of the heated chamber of the furnace. A water-cooled spout that locks into the mouth of the can was fabricated to convey the batch through the top of the furnace into the can.

With this new ICM arrangement, two melting runs were made using cans with radial heat transfer fins designed to increase heat transfer into each can while occupying no more than 10% of the can's volume. A melting rate of 50 kg/hr was easily sustained, and a 60 kg/hr rate was demonstrated in a 12-in.-dia can containing 10 fins of equal length. A melting rate of 90 kg/hr was demonstrated in a 20-in.-dia can containing 16 fins of special configuration. These can designs are being evaluated for defense waste vitrification applications.

FLUIDIZED-BED CALCINATION - J. C. Hartl

This quarter's progress comprises three significant developments:

- Defense-type wastes have been successfully calcined.
- Feed rates of 72 ℓ/hr have been demonstrated with the present fluidized-bed calciner, and operation at over 100 ℓ/hr seems possible. This corresponds to a specific feed rate of 250 to 300 $\ell/hr\text{-}ft^3$ of bed.
- Atomizing air rates have been reduced to one-fourth those previously used, significantly reducing the volume of noncondensible off gas. It is even possible that atomizing air may not be required at all.

The fluidized-bed calciner is being modified so that it can operate at approximately 100 ℓ/hr. The modifications include changes to the oxygen and kerosene systems and recalibration of some instrumentation. The unit is expected to be in operation by early November.

CANISTER DEVELOPMENT PROGRAM - S. C. Slate

This quarter we began a series of full-scale canister demonstrations using both in-can melter (ICM) and continuous melter (CM) systems. In a 10-day continuous run of the ICM system we filled ten 12-in.-dia canisters and two 16-in.-dia (304L stainless steel) canisters. These canisters have a twist-lock closure and were designed for bottom support. Eight carbon steel canisters were filled by the continuous melter. These canisters, which were 10 ft tall and ranged in diameter from 16 in. to 36 in., were the first full-sized canisters to be filled by this process.

Our analytical work has proceeded very well this quarter. We have developed a new transient thermal computer model of a canister and have analyzed its thermal performance in several different environments. We have also used this model to evaluate a variety of internal fin designs. Nine different fin designs have been fabricated and will be demonstrated in full-scale canisters.

The scope of the stress analysis work was expanded this quarter. We have also extended our capabilities to include some new analytical tools. Some of the important areas of work and accomplishments this quarter are summarized below:

- Wall thicknesses have been established for both ICM and CM canisters.
- The high-temperature creep tests of the 304L stainless steel and Inconel-601 have been completed.
- A large-scale canister creep test has been performed, and the results analyzed.[1]
- The subcooling method of reducing residual stress in glass canisters was demonstrated on lab-scale canisters.
- A thermal-structural and fracture mechanics analysis of the twist-lock canister closure system was made.
- A report entitled "High-Level Radioactive Waste Glass and Storage Canister Design" was released this quarter.[2] This report describes the design and evaluation activities at Pacific Northwest Laboratory concerning waste glass and canisters.

EFFLUENT STUDIES - M. S. Hanson

This quarter we completed, tested, and operated a common effluent system for use by all nonradioactive calciners and melters in the engineering development laboratory. The effluent train includes a venturi scrubber, a downdraft tube and shell condenser, a packed-bed scrubber, a mist eliminator, and a HEPA filter. The system has been successfully operated at spray calciner feed rates of over 200 ℓ/hr. The system provides for future installation of fission product adsorption beds and nitrogen oxide control devices.

In addition, we have set up and operated effluent characterization equipment on the nonradioactive effluent train. This equipment includes a classical aerosol scattering spectrometer and a gas chromatograph.

SECTION 2 - WASTE FORM CHARACTERIZATION

The purpose of waste form characterization is to measure the properties of candidate solidified products and containers (solidified waste and canister) as functions of composition, processing parameters, and storage conditions. The measurements are used to: 1) ensure operability of the vitrification processes and 2) provide data for safety analyses of high-level waste management. The ultimate goal of waste characterization is to characterize the physical and chemical properties of the waste forms so thoroughly that when they are placed in retrievable storage, and later in a final disposal site, we may be fully confident that their behavior is understood and that any changes or interactions with their environments are wholly predictable.

GLASS DEVELOPMENT - E. T. Sherman

A waste glass for the PW-7c-1 waste has been developed. We reported last quarter that melt 77-123 had been selected as the glass best suited for waste PW-7c-1. The composition of that melt has since been changed to improve resistance and decrease devitrification. The new waste glass for PW-7c-1 is 77-260. Its composition is:

SiO_2	36 wt%	Al_2O_3	2 wt%
Na_2O	8 wt%	TiO_2	6 wt%
B_2O_3	9 wt%	CuO	3 wt%
CaO	1 wt%	PW-7c-1	33 wt%
K_2O	2 wt%		

Melt 77-260 should be easily processed, since its viscosity is 30 poise at 1150°C, 90 poise at 1050°C, and 365 poise at 950°C.

The composition of 77-260 was varied to show the effect of compositional variations upon the homogeneity and leach rates of the vitreous product. The concentrations of B_2O_3, Na_2O, CaO, K_2O, CuO, and TiO_2 were varied plus or minus a few percent to simulate possible frit inconsistencies. Figure 1 shows the effects of these compositional changes on leach losses and homogeneity. The results show that B_2O_3 and Na_2O must be the most carefully controlled, since too much of either can cause high leach ratios, and too little can cause low viscosity. Variation of other oxides has very little effect upon the properties of the glass within the ranges tested.

Cadmium may be substituted for Gd as a soluble neutron poison during reprocessing. We made a glass similar to 77-260 in which Cd was substituted for Gd. This glass was fluid, homogeneous, and exhibited low leach losses of 0.12 wt% at pH 9 (16-hr test at 25°C), 0.18 wt% at pH 4 (19-hr test at 25°C), and 0.45 wt% in a Soxhlet apparatus (24-hr test at 99°C).

ENVIRONMENTAL REACTIONS OF WASTE GLASS - J. H. Westsik, Jr.

Comparison of Long-Term Leach Rates for Common Materials

Since the long-term, room-temperature leach test is used frequently to evaluate waste glasses, it was desirable to compare several common materials' durabilities in the same leach test. Similar comparison testing using the Soxhlet test was reported in previous PNL documents.[3,4]

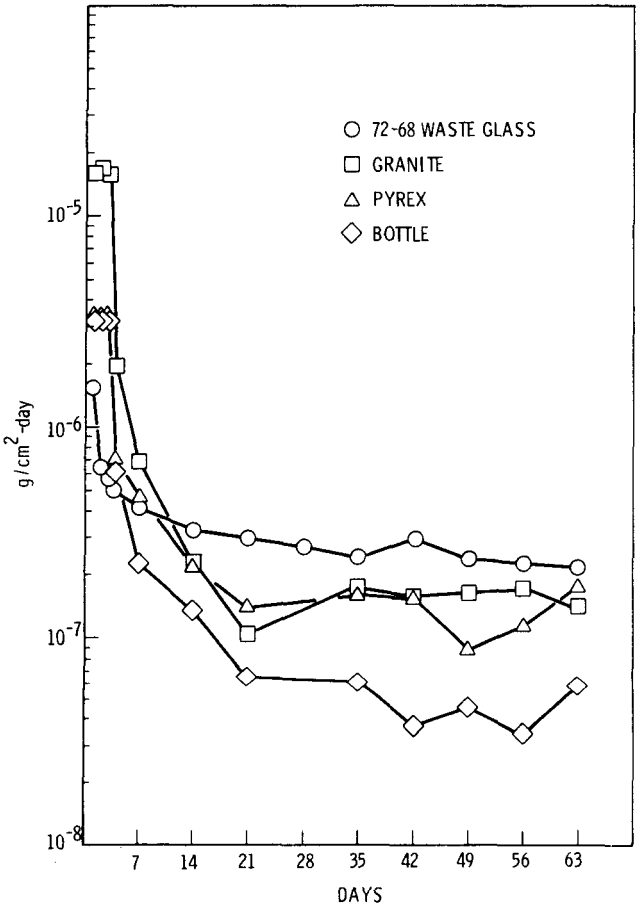

FIGURE 1. Long-Term Leach Rates of Common Materials

Samples of Pyrex glassware, bottle glass and granite were subjected to a modified IAEA long-term leach test procedure.(5) Sodium concentration in the deionized water leachant was monitored to determine the leach rates. Figure 2 shows the results of these tests along with the leach rate of 72-68 [Pw-4b-6(1:2.8)73-1] glass based on cesium behavior. The waste glass has durability similar to that of granite and Pyrex glass.

Leach Rates of Bulk vs Powdered Glass

Discrepancies between long-term leach rates of bulk and powdered samples of the same glass composition have been observed.(a)(6) Leach rates for simulated high-level waste (HLW) glass 72-68 were determined using -42+60 mesh granules; fully radioactive waste glass leach rates were measured using a disk of the glass. Full-level leach rates were about a hundred times higher than simulated glass leach rates.

This quarter we completed an experiment to determine whether the full-level glass leached faster because of radiation or because of the sample configuration. As Figure 2 illustrates, the difference is mainly due to the sample form. Leach rates of 72-68 glass

(a) Comparison of Figures 31 and 32 with Figure 60 in BNWL-2252 reveals this phenomenon.

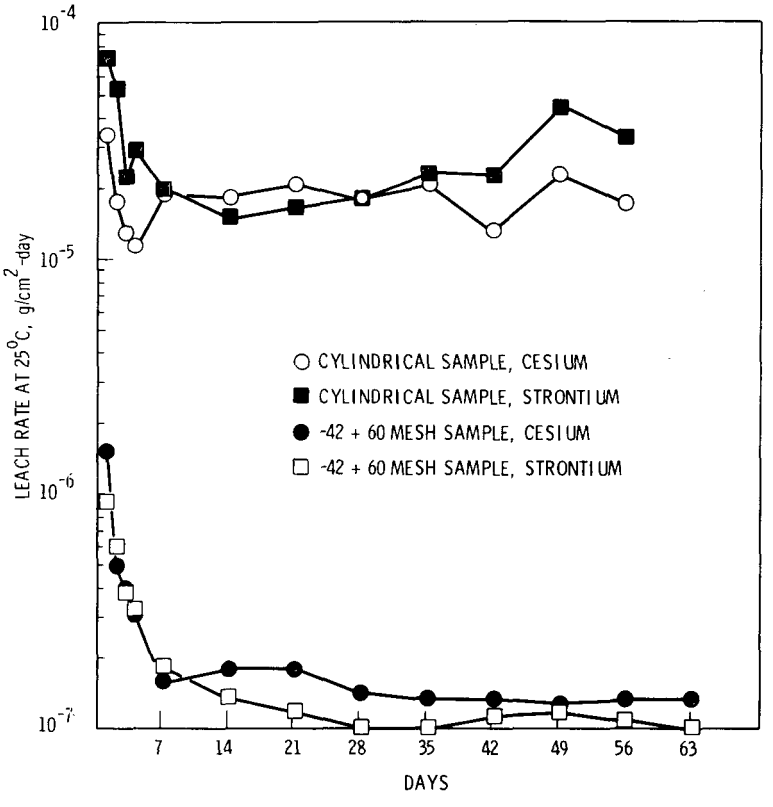

FIGURE 2. Long-Term Leach Rates for 72-68 Glasses

are shown for -42+60 mesh samples and core-drilled samples taken from the same piece of glass. The cored sample leaches faster by two orders of magnitude.

Theoretically, the powder should leach faster because of large pH increases in the interstitial solution. Apparently, some undetermined chemical and physical phenomena are overriding the expected effect.

LEACH RATES AT HIGH TEMPERATURES AND PRESSURES - J. H. Westsik, Jr.

This quarter we completed leach tests for various materials in a salt solution at 250°C and 1000 psi. During the 72-hr exposure period we measured weight loss to evaluate the durability. The data shown in Table 1 reveal that of all materials sampled the three metals have the highest apparent durability, although the length of exposure was not long enough to show the true corrosion behavior of the metals. The durabilities of the various ceramics and glasses fall within a narrow range. Within the limits of experimental error, the simulated HLW glasses and the nonirradiated light-water reactor (LWR) fuel pellet are at least as durable in the salt solution as is the National Bureau of Standards (NBS) borosilicate glass 717. The soda-lime-silica glass (NBS 710) had the highest leach rates.

We also conducted a series of tests to evaluate time effects on the durability of waste glasses. Samples of 76-68 glass were submerged in salt brine at 250°C and 1000 psi for periods of 3, 7, 14, and 21 days. The results, as shown in Figure 3, indicate that the glass reaches a maximum weight loss with no further losses after two weeks of leaching.

TABLE 1. Autoclave Salt Solution Leach Test Results(a)

Sample	Initial Weight, g	Geometric Surface Area, cm	Weight Loss Percent	Weight Loss g/cm^2-day
Soda-lime-silica glass NBS 710	6.1959	10.29	1.56	3.1×10^{-3}
72-68 [Pw-4b-7(1:2.8)73-1]	6.7115	8.93	0.29	7.2×10^{-4}
Granite	3.0511	5.795	0.36	6.4×10^{-4}
Borosilicate glass NBS 717	5.1363	10.12	0.31	5.2×10^{-4}
76-68 [Pw-8a-3(1:2)76-101]	6.9617	9.88	0.07	1.6×10^{-4}
Alumina	2.2770	4.32	0.088	1.5×10^{-4}
Nonirradiated LWR fuel pellet	9.4882	5.44	0.025	1.5×10^{-4}
Carbon steel	17.5736	12.64	0.02	7.4×10^{-5}
Inconel-601	19.0522	12.82	0.01	4.2×10^{-5}
304L stainless steel	9.2820	10.57	0.01	4.1×10^{-5}

(a) 72-hr tests done at 250°C and 1000 psi.

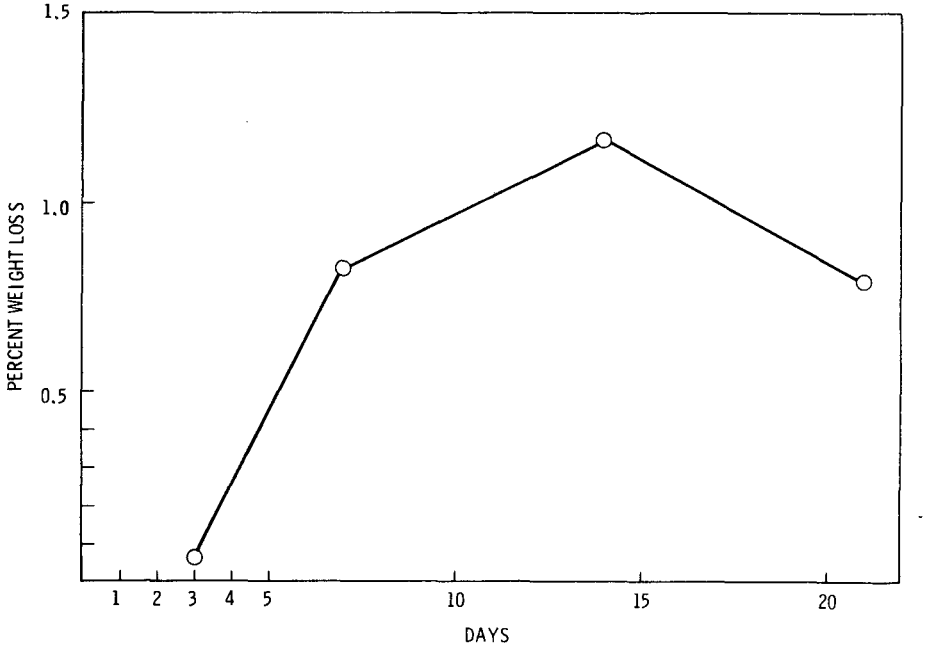

FIGURE 3. Chemical Durability of 76-68 Glass in Salt Brine at 250°C and 1000 psi

To date, autoclave testing indicates that higher temperatures accelerate waste glass corrosion. However, through reabsorption reactions or the achievement of equilibrium, the HLW glasses appear to achieve a chemical stability in the salt solution.

THERMAL EFFECTS UPON STORED GLASS - J. H. Westsik, Jr.

We have begun long-term anneals for glasses 77-107 [PW-9-3(1:2)77-268] and 77-260 [Pw-7c-3(1:2)77-269]. Waste glass 77-107 was melted at 1150°C before storage. Table 2 gives the composition for each of these two glasses; the annealing temperatures and times are shown in Table 3. After the glass samples have been stored for the times indicated, they will be air-quenched and tested for density, leach rates, and phase behaviors.

PHASE BEHAVIOR - R. P. Turcotte and J. W. Wald

Studies were performed this quarter to quantify the relationship between cooling rate and crystallization for the reference glass 72-68 and the glass 76-68. It was found that the two glasses vary significantly with respect to devitrification upon cooling. While the 76-68 glass can withstand cooling rates as slow as 6°C/hr from the processing temperature without significant increase in crystallinity, glass 72-68 must be cooled at a rate of about 50°C/hr or more to prevent crystallization. Thus, from a process standpoint, the 76-68 composition should be more suitable.

In addition, four fully radioactive waste glasses of four different representative compositions were prepared from full-level calcine, and have been produced in vitreous and devitrified conditions. To this point, optical examination has indicated that the glasses behave exactly as their nonradioactive counterparts do under similar conditions.

BULK AND THERMAL PROPERTIES OF WASTE GLASS - G. B. Mellinger

The densities of 76-68 and 77-260 glasses were measured as a function of temperature for temperatures ranging from 950° to 1300°C. The measurements were made by determining the bouyant force exerted on a 2-cm^3 platinum cylinder suspended in the molten glass. Using the density data, we were able to develop coefficients of thermal expansion (CTE) for these materials in this temperature range. Figure 4 graphs the relationship of temperature to the densities and CTEs of these glasses.

A preliminary apparatus for measuring the thermal conductivity of molten glass is being constructed. It will have a maximum temperature limit of 1000°C and will measure in the radial mode. We have ordered equipment that will measure the thermal conductivity of glass at temperatures up to 1300°C. We have also ordered instruments for measuring the electrical resistivity of molten waste glass.

THERMAL AND MECHANICAL SHOCK - L. R. Bunnell

Thermal Expansion

This quarter we completed work on a large number of waste glass samples taken from several canisters. The thermal expansion measurements were taken in air at a heating rate of 4°C/min to the softening point. Except as noted, the measurements were made on as-received, core-drilled specimens 0.4 in. in dia and 0.25 to 0.5 in. long. In all cases the diametral expansion was measured.

TABLE 2. Compositions of Glass 77-107 and Glass 77-260

Glass 77-107 PW-9-3(2:1)77-268		Glass 77-260 PW-7c-3(1:2)77-269	
Oxide	wt%	Oxide	wt%
Rb_2O	0.24	Rb_2O	0.11
SrO	0.70	SrO	0.29
Y_2O_3	0.39	Y_2O_3	0.17
ZrO_2	3.23	ZrO_2	1.50
MoO_3	4.30	MoO_3	1.95
RuO_2	2.15	RuO_2	0.86
Rh_2O_3	0.30	Rh_2O_3	0.16
PdO	1.15	PdO	0.49
Ag_2O	0.05	Ag_2O	0.02
CdO	0.08	CdO	0.03
TeO_2	0.49	TeO_2	0.22
Cs_2O	1.94	Cs_2O	0.79
BaO	1.10	BaO	0.55
La_2O_3	1.03	La_2O_3	0.45
CeO_2	2.33	CeO_2	0.91
Pr_2O_{11}	1.04	Pr_6O_{11}	0.44
Nd_2O_3	3.29	Nd_2O_3	1.48
Sm_2O_3	0.65	Sm_2O_3	0.33
Eu_2O_3	0.15	Eu_2O_3	0.06
Gd_2O_3	0.08	Gd_2O_3	10.31
U_3O_8	3.72	U_3O_8	5.27
Fe_2O_3	0.87	Fe_2O_3	1.21
Cr_2O_3	0.20	Cr_2O_3	0.02
NiO	0.08	NiO	0.01
Na_2O	5.37	Na_2O	11.13
P_2O_5	0.39	P_2O_5	2.35
SiO_2	37.81	MnO_2	0.11
B_2O_3	12.93	Zr fines	0.10
CaO	1.99	SiO_2	35.82
TiO_2	2.99	B_2O_3	8.95
K_2O	3.98	CaO	0.99
ZnO	4.97	K_2O	1.99
		Al_2O_3	1.99
		TiO_2	5.97
		CuO	2.99

TABLE 3. Waste Glass Sample Storage Matrix — Thermal Effects Studies

Temperature, °C	Storage Time					
	2 hr	1 Day	1 wk	2 mo	1 yr	5 yr
1200	X(a)					
1150	X					
1100	X					
1050	X					
1000	X					
900		X	X	X		
850		X	X	X		
800		X	X	X		
750		X	X	X	X	
700		X	X	X	X	
650		X	X	X	X	
600		X	X	X	X	
550		X	X	X	X	
500		X	X	X	X	X
400				X	X	X
300				X	X	X

(a) Each X represents one sample stored at the indicated temperature and time.

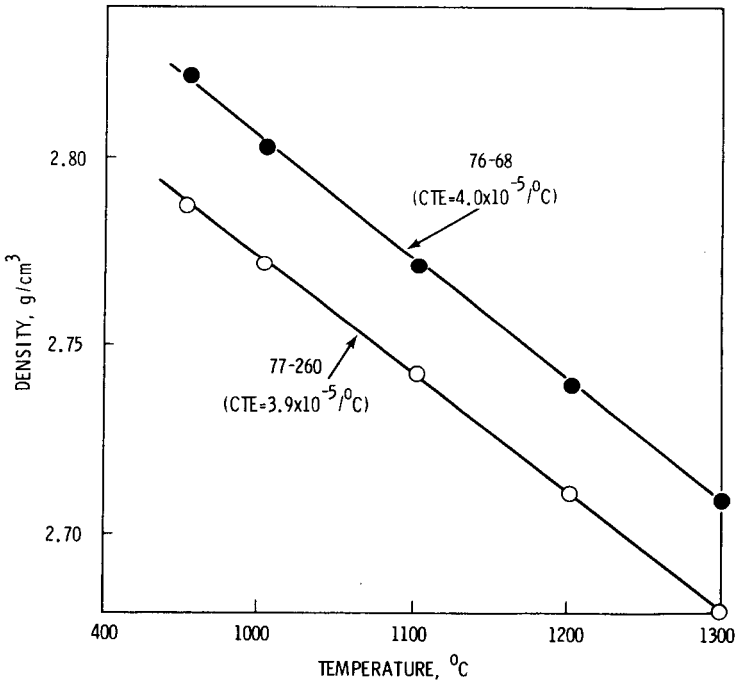

FIGURE 4. Density of 76-68 and 77-260 Waste Glasses as a Function of Temperature

Table 4 summarizes the data, showing expansion coefficients (25°to400°C), the glass transition (T_g), and the dilatometric softening point (T_s). Figures 5a, 5b, and 5c compile these parameters as a function of sample locations, and are intended to show trends.

TABLE 4. Thermal Expansion Parameters

Canister	Sample Location, in. from Bottom	Thermal Expansion Coefficient (25° to 400°C), $\alpha \times 10^{-6}/°C$	Glass Transition Temperature (T_g), °C	Glass Softening Point (T_s), °C
ICM-16	2-3	8.27	520	590
	6	9.47	517	555
	12	8.48	535	570
	18	7.92	535	595
	25	8.40	(a)	573
	28-30	8.53	531	565
ICM-18	0	9.33	515	545
	1	9.39	515	545
	6	8.67	520	552
	12	8.93	525	580
	18	9.07	515	555
	24	9.47	525	560
	28	10.53	(a)	550
ICM-21	0	9.33	525	565
	6	8.80	525	565
	12	9.07	530	563
	18	8.85	527	560
	24	6.40	525	558
ICM-23	0	9.60	525	625
	6	9.06	530	595
	12	10.0	533	575
	18	10.0	530	580
	24	9.47	525	595
ICM-20	0	8.93	545	585
	6	8.35	545	585
	12	8.21	545	590
	18	8.40	545	585
	24	8.53	540	570

(a) Indeterminate

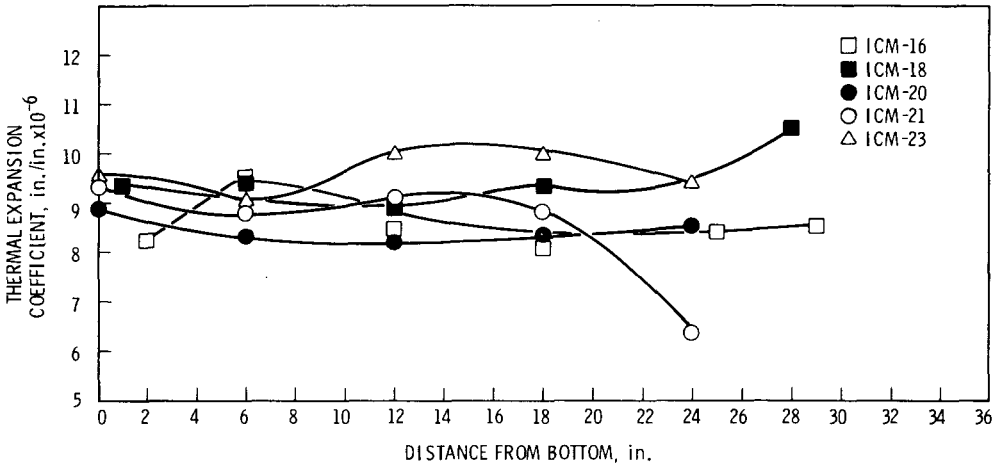

FIGURE 5a. Thermal Expansion Coefficient (α) for Five Glass Types as a Function of Distance from Canister Bottom

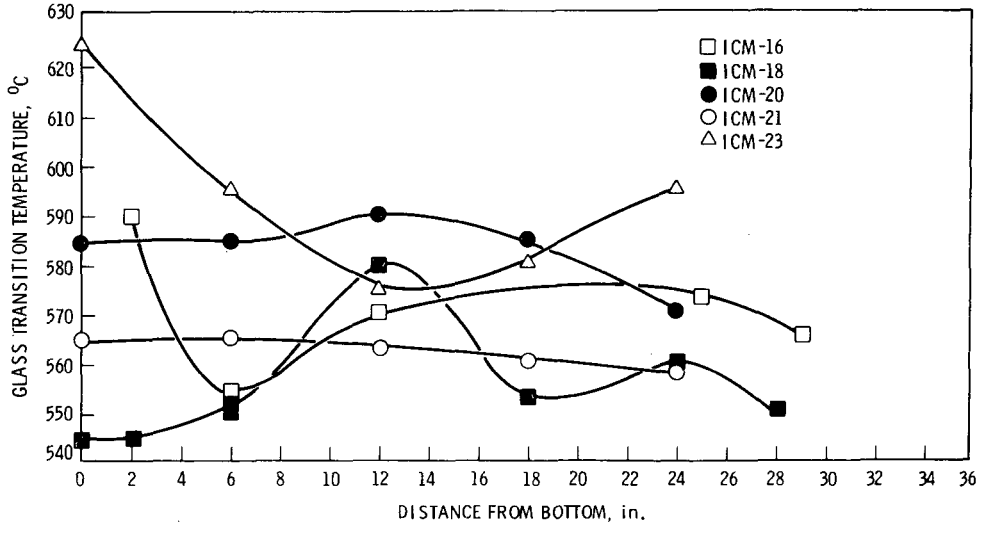

FIGURE 5b. Glass Transition Temperature (T_g) for Five Glass Types as a Function of Distance from Canister Bottom

In the case of In-Can Melter (ICM)-16, the specimens were taken within 0.5 in. of the canister wall, so the data may be influenced somewhat by thermal history effects. The expansion coefficient (α) is highest in the specimens taken 6 in. from the bottom of the canister, and is quite consistent at other locations. The high α is accompanied by decreases in both T_g and T_s, indicating a possible compositional shift at this location.

ICM-18 shows a gradual increase in α relating to increased distance from the canister bottom; T_g is constant within the accuracy of the measurements, and T_s peaks sharply 12 in. from the canister bottom.

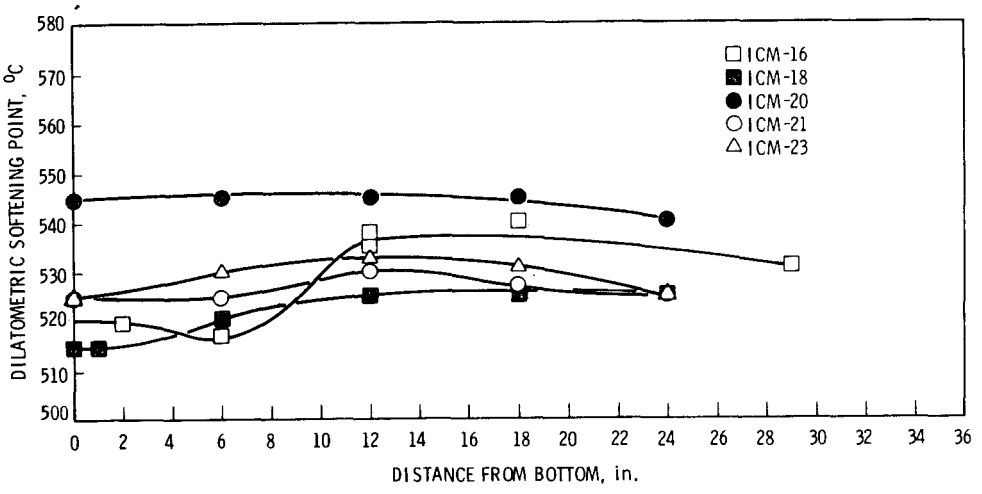

FIGURE 5c. Dilatometric Softening Point (T_S) for Five Glass Types as a Function of Distance from Canister Bottom

The parameters for ICM-20 were quite consistent throughout the canister, while ICM-21 showed an abnormally low thermal expansion at the top of the can, most likely representing a real composition change. ICM-23 was quite variable and showed a large change in T_S that is not reflected in the other two parameters. Since ICM-20, -21, and -23 were all sampled at random radial locations, thermal history variations again might be largely responsible for the changes noted.

Impact Testing

The impact testing done to date has utilized a machine capable of delivering a maximum of 160 ft-lb. Since the impact borne by the glass in a falling canister is much higher, and since a damage limit might be expected at high energies, the impact energy was increased an order of magnitude. This was done by mounting the impact punch, test specimen and die on the bottom of a 100-lb weight and dropping it onto a steel plate. In order to establish a tie point with data from the impact machine, the free-fall weight was tested at an identical drop height and energy. Data are presented in Figure 6 which show that the particles generated in free-fall impacts are somewhat finer, indicating that the energy is delivered to the specimen more efficiently in the free-fall apparatus.

The free-fall impactor was used to deliver 1400 ft-lb of energy to six specimens -- three of ICM-11 glass, and three of soda-lime-silica glass. These data are also shown in Figure 6. They indicate that a saturation limit has been reached and that the damage is no more severe in the higher-energy case. Surface area results are expected shortly, and will provide a better equation for the relationship between surface area and impact energy. To the previous limits of the energies used, the relationship has been quite linear.

In order to provide comparative impact data on a more recent glass composition than the ICM-11 used previously, specimens from ICM-23 were impacted recently. Results are plotted in Figure 7, and include ICM-11 and soda-lime-silica data for comparison. The

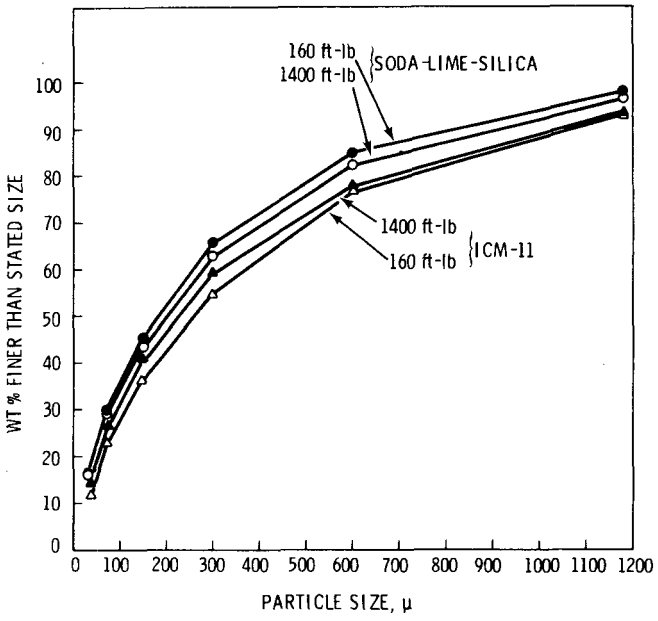

FIGURE 6. Particle Size Produced by 160 ft-lb and 1400 ft-lb Impacts Made by Free-Fall on Soda-Lime-Silica and ICM-11 Glasses

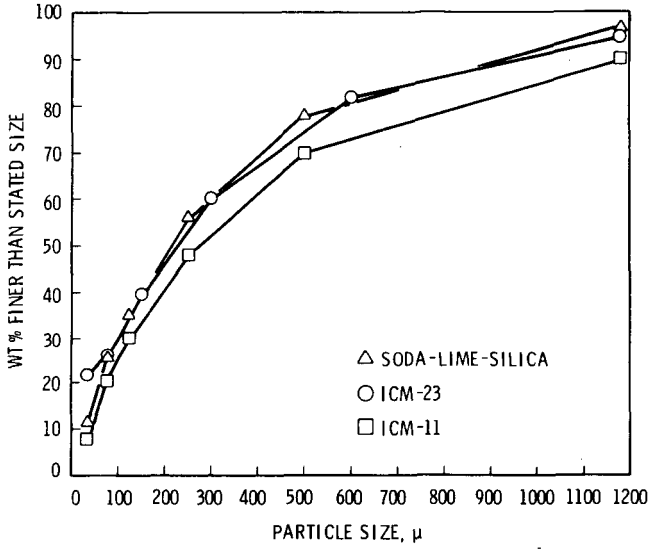

FIGURE 7. Particle Size Produced by 1600 ft-lb (Machine) Impacts for Soda-Lime-Silica, ICM-11, and ICM-23 Glasses

ICM-23 shows a somewhat poorer impact behavior than does ICM-11, especially in regard to production of fines. This might be attributed to the higher SiO_2 content in ICM-23 (38% vs ~25% for ICM-11). In the past we have found high silica content to correlate with high impact damage; fused silica is the worst performer tested thus far.

VAPORIZATION STUDIES - W. J. Gray

This quarter we began vaporization studies for 76-68 glass. Figure 8 is an Arrhenius plot and also shows data for two other glasses for comparison. Glass compositions are given in Table 5. Additional data for the two other glasses were published earlier.[7,8]

Of the waste materials we have studied, glass 76-68 is the first to show a nonlinear Arrhenius plot. Actually, linear behavior seems unlikely for such complex systems. Perhaps because cesium is by far the dominant vapor species, it usually overrides everything else and gives rise to the linear Arrhenius plots. Figure 8 shows that the relative weight losses of the three glasses follow the same order as do their cesium concentrations, suggesting another manifestation of the dominance of cesium volatility in relation to all other tested elements.

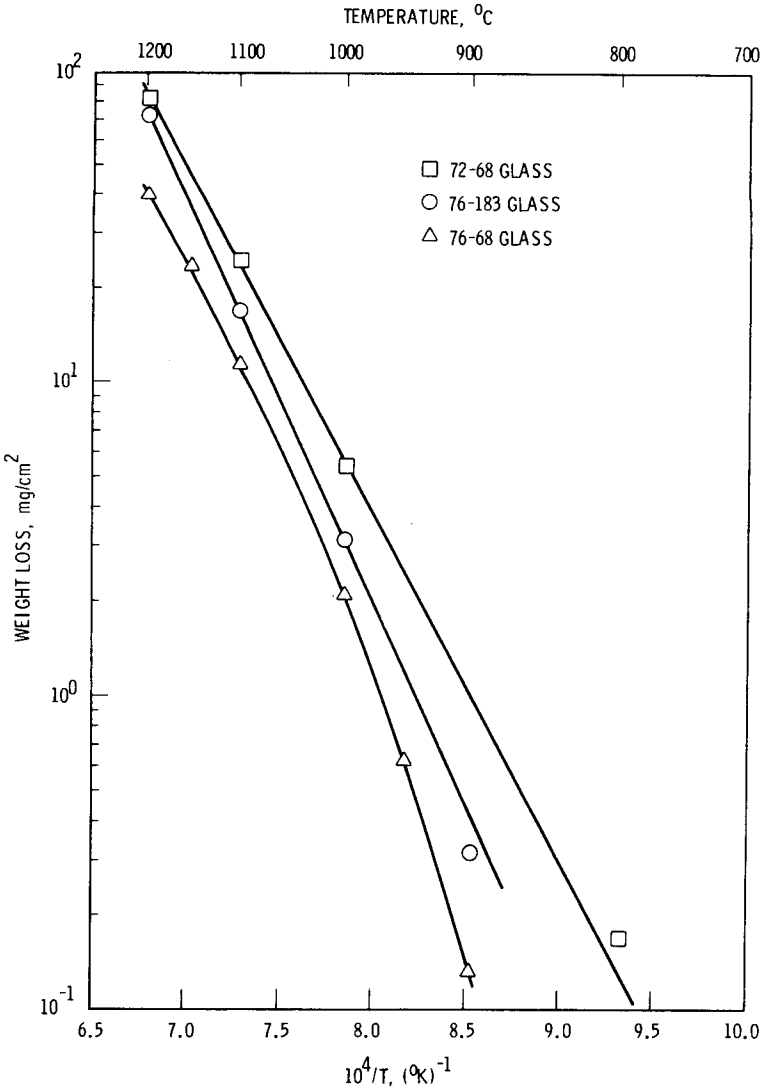

FIGURE 8. Weight Loss After 12 hr in Dry Air

TABLE 5. Waste Glass Compositions

Constituent	Nominal Concentration, wt% 72-68	76-183	76-68
Glass frit			
B_2O_3	11.30	9.50	9.47
Na_2O	4.12	8.00	--
MgO	1.50	--	--
Al_2O_3	--	1.00	--
SiO_2	27.71	35.50	39.80
K_2O	4.12	2.0	--
CaO	1.50	2.00	2.00
TiO_2	--	6.00	2.97
CuO	--	3.00	--
ZnO	21.64	--	4.97
SrO	1.50	--	--
BaO	1.50	--	--
Inerts			
Na_2O	--	3.64	12.80
P_2O_5	0.44	3.36	0.51
Cr_2O_3	0.23	0.19	0.44
Fe_2O_3	1.00	1.60	10.34
NiO	0.09	0.56	0.21
Gd_2O_3	--	5.49	--
Fission products			
Rb_2O	0.23	0.19	0.13
SrO	0.70	0.56	0.40
ZrO_2	3.28	2.62	1.88
MoO_3	4.29	3.38	2.42
RuO_2	1.97	1.57	1.13
Rh_2O_3	0.32	0.16[a]	0.18
PdO	0.98	--	0.56
Ag_2O	0.06	0.05	0.03
CdO	0.06	0.05	0.04
TeO_2	0.48	0.39	0.28
Cs_2O	1.91	1.53	1.09
BaO	1.04	0.83	0.59
$Y+RE_2O_3$	8.03	6.85	7.76

(a) Co substituted for Rh.

SECTION 3 - ALTERNATIVE WASTE FIXATION PROCESSES

The goal of this task is to develop alternative waste fixation procedures that will serve as viable backup processes. Cost and safety factors of the alternative processes and products are to be compared to those of the current reference process and product--silicate glass castings in large metal canisters. These alternative processes are being developed on the laboratory scale. In the concept currently emphasized the waste is formed into small granules or pellets that are coated with nonradioactive, inert materials to provide containment and leach resistance. The coated waste shapes are then incorporated into a metal matrix that provides impact resistance and increased thermal conductivity.

GLASS MARBLE DEVELOPMENT - J. M. Rusin

Figure 9a illustrates the reaction zone observed in Pb-encapsulated waste glass marbles that were heat-treated at 300°C for 10 days. Energy dispersive analysis showed that the zone contained only Pb. As there is a 40 μm gap between the marble and the matrix, the reaction zone is probably an oxide of Pb.

The reaction zone is much more complex for the Pb-encapsulated waste glass marbles heat-treated at 500°C for 10 days. At least two phases are observed, as shown in Figure 9b. The needle-like phase has a high Zn and Pb content, along with trace amounts of rare earths. The lighter areas have a high Pb content (probably lead oxide), whereas the rest of the reaction zone contains both Pb and elements contained in the glass.

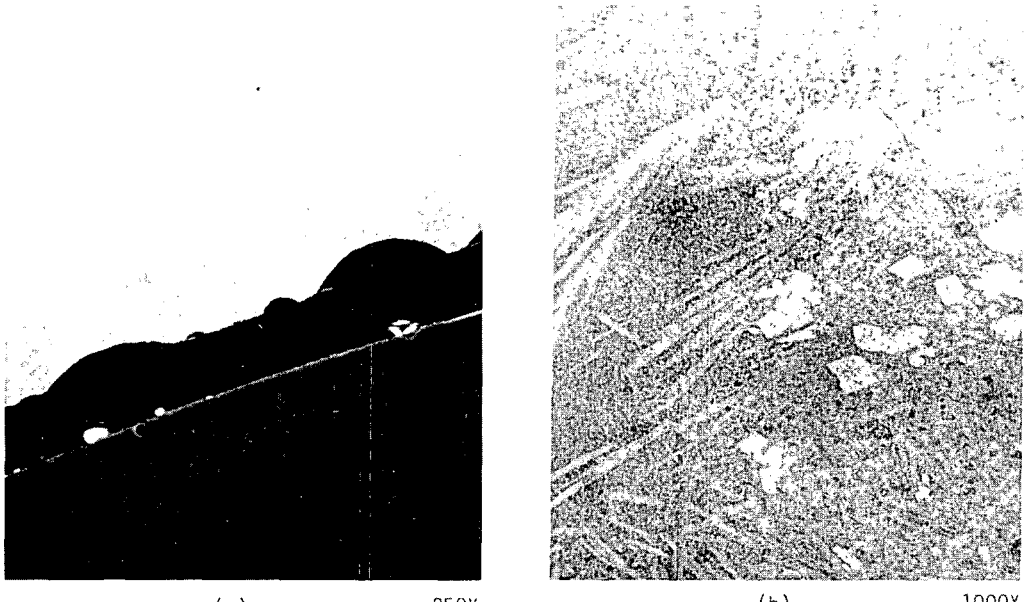

(a) 250X (b) 1000X

FIGURE 9a,b. Reaction Zones in Heat-Treated Pb-Encapsulated Waste Glass Marbles

The above results have only confirmed why a Pb-10Sn alloy has been selected. Previous experiments had shown that molten Pb would react with waste glass, but other studies demonstrated that even while molten at 500°C, a Pb-10Sn alloy will not react with waste glass.

SUPERCALCINE - G. J. McCarthy, The Pennsylvania State University

The nature of the Penn State participation in the development of alternative waste forms and the Supercalcine concept has been described in previous reports. Current objectives of the Supercalcine Task include: 1) refinement of existing formulations for PW-4b and PW-7 wastes, 2) development of formulations for the high-sodium waste, PW-7a, 3) determination of crystalline phase behavior of cesium, ruthenium, tellurium, palladium, rhodium, and the actinides in Supercalcine, and 4) consideration of the effects of radiation and transmutation on Supercalcine stability.

Some of the highlights of this quarter's work are listed below:

- We completed a comprehensive study on phase-pure $CsAlSiO_4$ and $CsAlSi_2O_6$ preparation. In doing so, we surveyed 18 combinations of starting materials and four firing temperatures, and found the optimum methods of preparing these phases.
- We completed a thorough literature review of crystal chemical and phase equilibria data on portions of the system U-Th-Ce-Zr-RE-O relevant to the Supercalcine phases F_{ss} and T_{ss}. The articles and reports are now being studied and correlated in preparation for experimental studies on poorly represented areas of this system vital to defining phase behavior in F_{ss} and T_{ss}.
- We began a definitive study of ruthenium's role in the thermal stability of Supercalcine. Volatilization weight losses normalized to surface area in 10% Ru-loaded SPC-2 and fully loaded SPC-2 are being compared using TGA and static firings of varying durations.

The balance of this report will focus upon phase behavior in the developmental "dirty" (high-Na) Supercalcines 77-2 and 77-3 and in the PNL engineering-scale formulation SPC-4.

Phase Behavior in High-Sodium Supercalcines 77-2 and 77-3

Refer to the last report for the crystalline phase formation models of these formulations.[9] The phases observed by x-ray diffraction in the products of the routine air firings are listed in Table 6 below (in order of decreasing relative intensity in the diffractograms).

The new and unexpected phase occurring in the products of the 1000°C firings was tentatively identified as $Na_2U_2O_7$ (PDF 26-973) by searching the Powder Diffraction File. We confirmed the identification by synthesizing the pure phase--starting with nitrate solutions of Na and U and repeating the Supercalcine experimental conditions.[a]

It is apparent that at lower temperatures Na combines with U to form the $Na_2U_2O_7$ phase, but at temperatures approaching 1100°C Na has a greater affinity for the aluminosilicate sodalite phase and U forms in the fluorite phase. Valence change accompanies

(a) Also, a recent paper from ANL[10] reports the routine preparation of $Na_2U_2O_7$ in air from Na_2CO_2 + U_2O at 800° to 850°C.

TABLE 6. Phases Observed by X-ray Diffraction in Air-Firing Products from High-Sodium Supercalcines

Air-Firing Conditions	Supercalcine(a) 77-2	Supercalcine(a) 77-3
0.5 in. pellets at 1000°C for 2 hr	S-F_{ss} (5.36Å)	S-$Na_2U_2O_7$
	MS-So_{ss}	S-M_{ss}
	M-$Na_2U_2O_7$	S-So_{ss}
	MW-T	MW-T_{ss}
	MW-P	MW-F_{ss} (5.37Å)
		W-P
0.5 in. pellets at 1100°C for 2 hr	VS-F_{ss} (5.36Å)	S-F_{ss} (5.36Å)
	S-So_{ss}	MS-M_{ss}
	M-M_{ss}	M-So_{ss}
	M-T_{ss}	MW-T_{ss}
	W-P	VW-$Na_2U_2O_7$

(a) Phases rated in order of decreasing relative intensity in the diffractograms: S = strong, M = medium, W = weak, V = very. Phases are abbreviated as follows:

F_{ss} = Fluorite $[(U,Ce,Zr, Re^{3+}...)O_{2+x}]$

So_{ss} = Sodalite $[(Ca,Sr,Ba)_{2-x}[NaAlSiO_4]_6 (MoO_4)_{2-x}]$

M_{ss} = Monazite $[REPO_4]$

T_{ss} = Tetragonal Zirconia $[(Zr,...)O_{2+x}]$

P_{ss} = Pollucite $[(Cs,Rb,Na)AlSi_2O_6]$

these phase changes, since U is hexavalent in $Na_2U_2O_7$ but is predominantly tetravalent in F_{ss}. We expect that the U (and associated Pu) in this $Na_2U_2O_7$ would be more leachable than U in F_{ss}, so crystallization of this phase should be avoided by using the higher firing temperatures.

X-ray analysis of the specimens that were used in the 14-day Soxhlet leaching tests did not show any changes in phase assemblages or any reduction in the intensities of reflections that would be expected if a phase or phases were being preferentially leached. The products of the 21-day, 800°C thermal stability tests showed increased crystallinity, as would be expected, but no changes in x-ray phase assemblage.

Phase Formational Model for Supercalcine SPC-4

A spray calciner run of a PW-7-based Supercalcine SPC-4 was performed at PNL this spring. The phase formation model of SPC-4 is shown in Table 7.

CORE AND GLASS FRIT COATING - J. M. Lukacs and C. B. Ruhter

This quarter spray calcined SPC-4 powder was agglomerated by the disc pelletizer into spherical pellets 4 mm to 15 mm in dia using water as binder. Pellet green strength was

TABLE 7. Phase Formation Model of SPC-4

PW-7 Ions, mmol	Desired Phase, mmol	Additives, mmol
257 (RE + Ce)[a]	32.1 $Ca_2RE_8(SiO_4)_6O_2$,[A_{ss}]	64 Ca 193 Si
100 [PO_4]	100 $REPO_4$,[M_{ss}]	--
100 RE		--
106 Zr	106 Tetragonal-ZrO_2,[T_{ss}]	--
54 Ba+Sr	95 $(Sr,Ba)MoO_4$,[S_{ss}]	41 Sr
95 Mo		
54 Cs	74 $(Cs,Rb,Na)AlSi_2O_6$,[P]	128 Si
10 Rb		
10 Na		
100 Fe	$(Fe,Cr)_2O_3$,[$(Fe_2O_3)_{ss}$]	--
12 Cr	plus	--
5 Ni	$(Ni,Fe)(Fe,Cr)_2O_4$,[SP_{ss}]	--
6 Ru	in RuO_2 and A_{ss}	
2 Cd		
2 Ag		

(a) Some Ce and RE are expected to crystallize with Zr in a F_{ss} phase during firings in air. If SPC-4 is fired in an inert or reducing atmosphere, the F_{ss} phase may not crystallize.

sufficient to withstand handling and transfer steps with minimal breakage. Sintering at 1230°C for 2 hr produced dense, hard pellets with a bulk packing density of 2.36 to 2.44 kg/ℓ. Nine kilograms of sintered pellets were processed.

One liter of sintered pellets was manually coated with a glaze slip (Ferro CM-850). After drying, the coatings were vitrified by placing the pellets in a 1000°C furnace for 5 minutes.

Dusting of the fine Supercalcine powder has been a recurrent problem with the disc pelletizer. The installation of a hood over a portion of the pelletizer and the use of a dust collector has greatly reduced process dusting.

CHEMICAL VAPOR DEPOSITED COATINGS - M. F. Browning[a]

The application of a SiO_2 coating was tested as a method of preventing oxidation of the PyC precoat, as occurs when Al_2O_3 coatings are applied because of the CO_2 reactant employed. Silicon dioxide coating by the pyrolysis of tetraethyorthosilicate, which involves an essentially nonoxidizing environment, was successfully accomplished without loss to the PyC layer. Unfortunately, the coatings could not be made sufficiently

(a) Battelle, Columbus Laboratories

protective, even when applied at 1000°C to thicknesses of 90 μm. The coatings did not crack during the oxidation test at 750°C, but appeared to contain some surface-connected porosity.

The Al_2O_3 and SiO_2 coating systems were then combined in an attempt to prepare dual coatings in a drum coater. We developed a procedure for accomplishing the application of a SiO_2/Al_2O_3 coating. Particles (SPC-2, 3- to 5-mm, heated for 6 hr at 1125°C in air) were coated with 40 μm of PyC, ∿16 μm of SiO_2, and finally ∿50 μm of Al_2O_3. Oxidation of a sample of this material at 750°C in air for 89 hr confirmed that the outer Al_2O_3 coating was impervious, in that weight loss amounted to only 0.02%. Complete loss of the PyC would give a weight change of ∿1%.

This quarter we also developed a second successful approach to applying a dense Al_2O_3 coating over PyC by a reaction involving $CO_2 + H_2$. This was in connection with the development of larger-capacity coating systems. We determined that ∿10 μm of Al_2O_3 applied to the PyC using a water vapor hydrolysis reactant instead of $CO_2 + H_2$ would protect the PyC during the application of the remainder of the Al_2O_3 coating using $CO_2 + H_2$. Although this approach was developed for use in a vibrating bed system, it should also be suitable for use with a drum coating system.

Two new larger-capacity coating systems were developed during this report period. The PyC system consists of a 53-mm quartz fluidized-bed reactor with a typical cone-bottom support. The system was operated in a fluidized-bed mode using a bed dilutent of ZrO_2 (25 to 40 mesh) to ensure that the larger Supercalcined particles were well agitated. PyC coatings were typically deposited at ∿1100°C from a 50:50 acetylene/argon mixture at a rate of ∿1.5 μm/min. The capacity of the system is roughly 100 cm^3 of product per run for a coating thickness of 40 to 50 μm.

The coating system we have set up for applying Al_2O_3 to the PyC-coated particles also has a production capacity of roughly 100 cm^3. A coating reactor of 37-mm quartz with a hemispherical bed support was used. Aluminum chloride was formed in situ in a section below the bed support by the hydrochlorination of aluminum. We introduced carbon dioxide and hydrogen or water vapor into the system through a centrally positioned tube extending from the top of the reactor and terminating in the particle bed. A new mechanical vibrator was installed which imparted a vertical vibratory motion to the reactor and thus to the particles. The resulting particle agitation was strong enough to yield a reasonably uniform coating on each particle without operating in a fluidized-bed mode or using a bed dilutent. This obviously has the advantages of: 1) requiring much less total gas flow, and 2) providing greater usable product capacity. Dense, smooth Al_2O_3 coatings of 30 to 40 μm were typically deposited at ∿1050°C at a rate of roughly 4 to 5 μm/hr.

METAL MATRIX DEVELOPMENT - R. O. Lokken, K. R. Sump, and C. B. Ruhter

We have conducted sintering studies on small samples of a ^{90}Cu-10Sn bronze to determine if this material could satisfy the sintering requirements and limitations of glass-coated Supercalcine. Sintering temperatures studied were 500°C, 550°C, 600°C,

670°C, and 700°C. The lowest three temperatures resulted in limited sintering, with the outer layers of powder easily removed by light abrasion. Samples sintered at 670°C and 700°C demonstrated good sintering characteristics. It should be noted, however, that all samples were sintered for 6 hr in air; thus, the formation of oxides may affect the overall sintering characteristics. We are currently doing studies to determine sintering characteristics of bronze in a dynamic vacuum.

The 1-ℓ canisters have been received for the waste-form encapsulation demonstrations. We have encapsulated simulated waste glass marbles and 6-mm glass beads in a Pb-10Sn matrix by vacuum casting. A vacuum tube is welded to the canister near the bottom. A second, closed-end tube, welded to the top of the canister, is used for the access of molten metal. The canister of simulated waste glass marbles was preheated to ∿350°C under a dynamic vacuum, then submerged in a crucible of molten Pb-10Sn at 400°C. The tube on the top of the canister was broken off and the Pb-10Sn filled the canister. The canister was then removed from the crucible and allowed to air cool.

While this method of encapsulation provides for good filling of the voids between marbles, it has certain drawbacks. As the canister is removed from the crucible at 400°C, the supply of molten metal is cut off. As the canister cools and the Pb-10Sn begins to solidify, shrinkage begins to occur, resulting in a shrinkage cavity at the top of the canister. Alleviating this problem requires an additional supply of molten metal to fill the volume of the cavity.

CHARACTERIZATION - J. M. Rusin

Impact Behavior

We have determined surface areas for impacted 3-mm and 6-mm glass beads and 1-mm alumina beads. Results are plotted in Figure 10 and listed in Table 8. The beads were contained in a 0.5-in.-dia by 0.5-in.-high cavity during impact. The surface area created as a function of impact energy is also listed in Table 8. It appears that the impact behavior of alumina beads may differ from that of glass beads. The results are plotted in Figure 11 for comparison.

Reactions Between Supercalcine and Metal Matrices

No reactions were detected by SEM analysis for uncoated Supercalcine encapsulated in vacuum-cast Pb-10Sn and Al-12Si and in gravity-sintered Cu. Reactions were observed, however, for uncoated Supercalcine in gravity-sintered 316 SS.

A second phase was observed in the Al-12Si matrix that contained Al, Si, V, Cr, and Fe. In the Pb-Sn matrix there were some single-phase Sn regions similar to those previously observed in Pb-Sn matrices.

The bonding between Cu spheres in the gravity-sintered Cu sample was minimal. We observed very little neck growth, as shown in Figure 12. Flux coating is being investigated to improve the bonding. During encapsulation the fused silica tube containing the Cu sample developed a white reaction zone next to the Cu. This has been shown to be cristobalite by thin section microscopy studies.

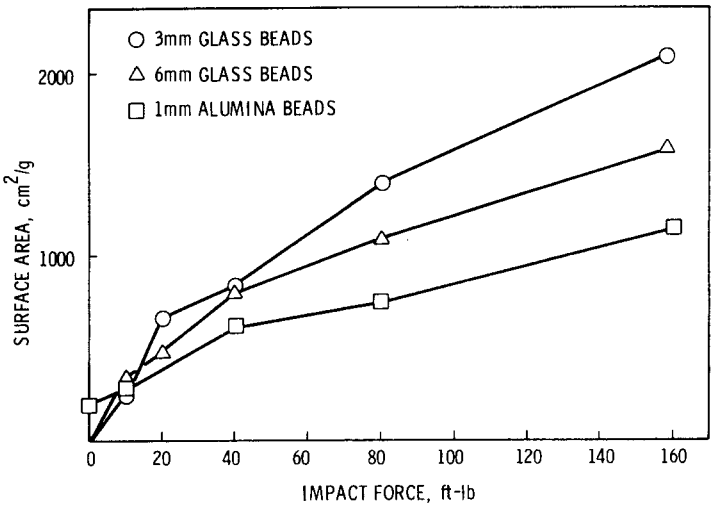

FIGURE 10. Surface Area vs Impact Force for Glass and Alumina Beads

TABLE 8. Effect of Impact Force Upon Surface Area

Sample	Impact Force, ft-lb	Surface Area, cm^2/gm	Increase in Surface Area, cm^2/gm	Increased Surface Area/Imparted Energy, cm^2/joule
3-mm glass beads	0	8	0	--
	9.9	250	242	52.97
	19.8	670	662	72.45
	39.6	840	832	45.52
	79.2	1400	1392	38.08
	158.4	2100	2092	28.62
6-mm glass beads	0	4	0	--
	9.9	340	336	72.22
	19.8	490	486	52.23
	39.6	820	816	43.84
	79.2	1100	1096	29.44
	158.4	1900	1896	25.47
1-mm alumina beads	0	200	0	--
	9.9	270	70	23.38
	39.6	620	420	36.90
	79.2	745	545	22.75
	158.4	1370	1170	24.23

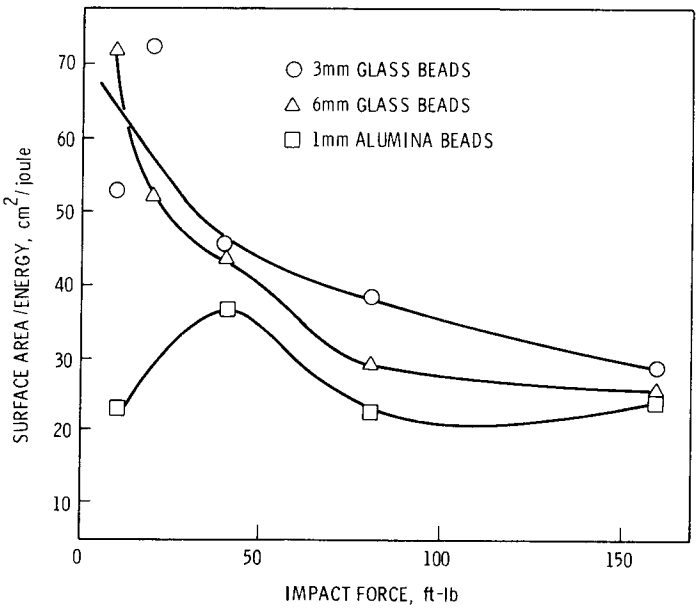

FIGURE 11. Surface Area/Impact Energy Coefficient vs Impact Force for Glass and Alumina Beads

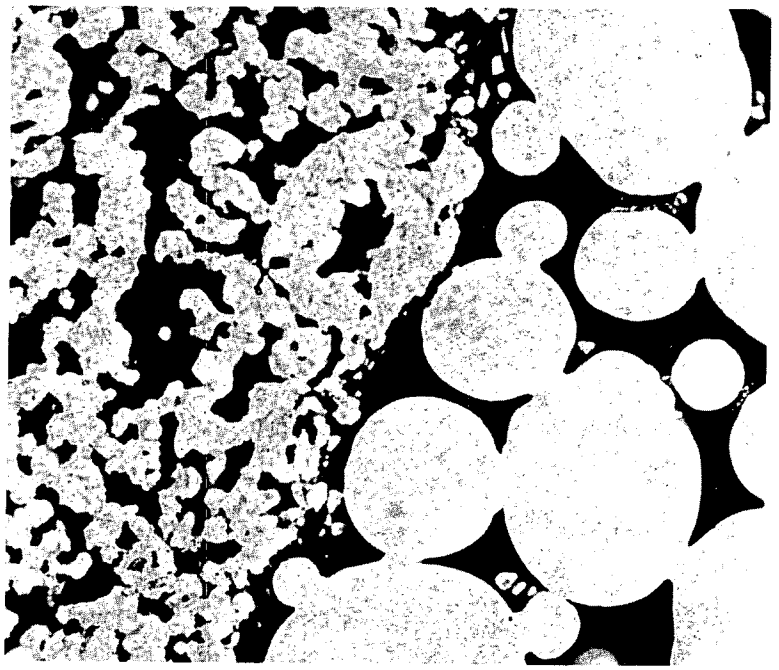

FIGURE 12. Uncoated Supercalcine Cores in Gravity-Sintered Copper

The gravity-sintered 316 SS sample had a reaction zone around the stainless steel particles, as shown in Figure 13. Dispersive energy analyses of the white area (labeled a) and the darker crystalline area (labeled b) were conducted. The white area has high Mo, Cr, and Fe contents, whereas the darker crystalline region surrounding the SS particle is primarily Cr. Samples of coated Supercalcine encapsulated in gravity-sintered 316 SS do not contain any of the above observed phases. This, along with vaporization studies which show that a considerable amount of Mo is vaporized, leads us to conclude that the observed reaction products may be caused by Supercalcine vaporization. Thus, if Supercalcine is to be encapsulated at higher temperatures, a coating may be necessary.

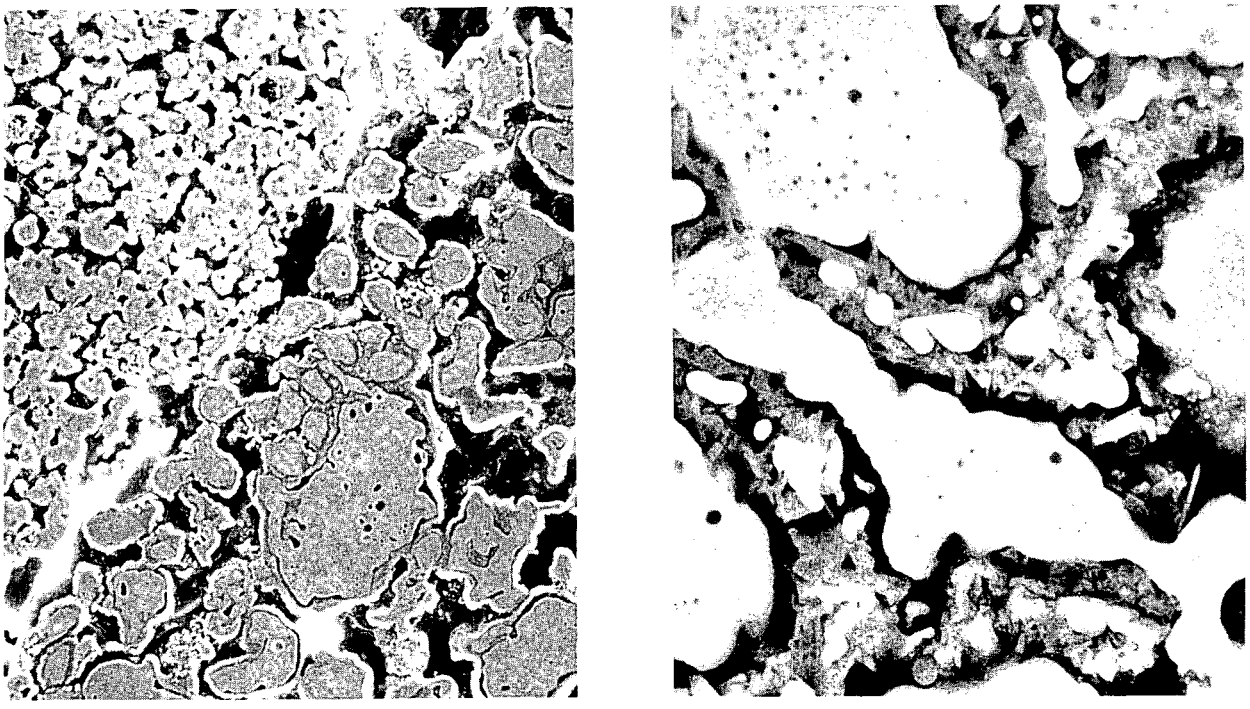

(a) 300X (b) 3000X

FIGURE 13 a,b. Uncoated Supercalcine Cores Encapsulated in Gravity-Sintered 316 SS

REFERENCES

1. Simonen, F. A. and S. C. Slate. 1977. Creep Analysis of Canisters for Radioactive Waste Vitrification. BNWL-SA-6351, Pacific Northwest Laboratory, Richland, WA 99352.

2. Slate, S. C. and W. A. Ross. 1977. High-Level Radioactive Waste Glass and Storage Canister Design. BNWL-SA-6379, Pacific Northwest Laboratory, Richland, WA 99352.

3. McElroy, J. L. et al. 1975. Quarterly Progress Report - Research and Development Activities Waste Fixation Program - April Through June 1975. BNWL-1932, Pacific Northwest Laboratory, Richland, WA 99352.

4. Platt, A. M. et al. 1973. Quarterly Progress Report - Research and Development Activities Waste Fixation Program - December 1972 Through March 1973. BNWL-1741, Pacific Northwest Laboratory, Richland, WA 99352.

5. Hespe, E. D. 1971. "Leach Testing of Immobilized Radioactive Waste Solids, A Proposal for a Standard Method." Atomic Energy Review. 9:1.

6. Mendel, J.E. et al. 1977. Annual Report on the Characteristics of High-Level Waste Glasses. BNWL-2252, Pacific Northwest Laboratory, Richland, WA 99352.

7. Gray, W. J. 1976. Volatility of a Zinc Borosilicate Glass Containing Simulated High-Level Radioactive Waste, BNWL-2111, Pacific Northwest Laboratory, Richland, WA 99352.

8. McElroy, J. L. et al. 1977. Quarterly Progress Report - Research and Development Activities Waste Fixation Program - January Through March 1977, PNL-2265-1, Pacific Northwest Laboratory, Richland, WA 99352.

9. McElroy, J. L. 1978. Quarterly Progress Report - Research and Development Activities Waste Fixation Program - April Through June 1977, PNL-2265-2, Pacific Northwest Laboratory, Richland, WA 99352.

10. Lyon, W. G. et al. 1977. Journal of Chemical Thermodynamics. 9:201.

DISTRIBUTION

No. of Copies

UNITED STATES

A. A. Churm
DOE Chicago Patent Division
9800 South Cass Avenue
Argonne, IL 60439

R. E. Cunningham
Deputy Director for Fuels and Materials
Nuclear Regulatory Commission
Silver Springs, MD 20910

Assistant Director for Radioactive Waste Management Branch
NRC Division of Materials and Fuel Cycle Facility Licensing
Washington, DC 20545

W. G. Belter
DOE Division of Biomedical and Environmental Research
Earth Sciences Branch
Washington, DC 20545

W. A. Brobst
DOE Division of Environmental Control Technology
Washington, DC 20545

W. E. Mott
DOE Division of Environmental Control Technology
Washington, DC 20545

R. B. Chitwood
DOE Division of Nuclear Power Development
Washington, DC 20545

T. C. Chee
DOE Office of Nuclear Waste Management
Washington, DC 20545

C. R. Cooley
DOE Office of Nuclear Waste Management
Washington, DC 20545

Sheldon Meyer
DOE Office of Nuclear Waste Management
Washington, DC 20545

R. G. Romatowski
DOE Office of Nuclear Waste Management
Washington, DC 20545

C. W. Kuhlman
DOE Office of Nuclear Waste Management
Washington, DC 20545

No. of Copies

C. A. Heath
DOE Office of Nuclear Waste Management
Washington, DC 20545

G. Oertel
DOE Office of Nuclear Waste Management
Washington, DC 20545

A. F. Perge
DOE Office of Nuclear Waste Management
Washington, DC 20545

W. S. Scheib, Jr.
DOE Office of Nuclear Waste Management
Washington, DC 20545

D. L. Vieth
DOE Office of Nuclear Waste Management
Washington, DC 20545

R. D. Walton
DOE Office of Nuclear Waste Management
Washington, DC 20545

J. Neff, Program Manager
Department of Energy
Columbus Program Office
505 King Avenue
Columbus, OH 43201

J. B. Whitsett
DOE Idaho Operations Office
P.O. Box 2108
Idaho Falls, ID 83401

J. J. Schreiber
DOE Oak Ridge Operations Office
P.O. Box X
Oak Ridge, TN 37830

John Van Cleve
DOE Oak Ridge Operations Office
P.O. Box X
Oak Ridge, TN 37830

E. S. Goldberg
DOE Savannah River Operations Office
P.O. Box A
Aiken, SC 29801

334 DOE Technical Information Center

A. P. Roeh, Manager
Allied Chemical Corporation
550 2nd Street
Idaho Falls, ID 83401

No. of
Copies

J. R. Berreth
Allied Chemical Corporation
550 2nd Street
Idaho Falls, ID 83401

R. A. Brown
Allied Chemical Corporation
550 2nd Street
Idaho Falls, ID 83401

C. A. Hawley
Allied Chemical Corporation
550 2nd Street
Idaho Falls, ID 83401

D. A. Knecht
Allied Chemical Corporation
550 2nd Street
Idaho Falls, ID 83401

Allied Chemical Corporation
(File Copy)
550 2nd Street
Idaho Falls, ID 83401

M. D. McCormack
E.G.&G.Idaho, Inc.
P.O. Box 1625
Idaho Falls, ID 83401

W. C. Seymour
E.G.&G. Idaho, Inc.
P.O. Box 1625
Idaho Falls, ID 83401

R. A. Buckham
Allied-General Nuclear Service
P.O. Box 847
Barnwell, SC 29812

A. Williams
Allied-General Nuclear Service
P.O. Box 847
Barnwell, SC 29812

J. L. Jardine
Argonne National Laboratory
9700 South Cass Avenue
Argonne, IL 60439

M. M. Steindler/L. E. Trevorrow
Argonne National Laboratory
9700 South Cass Avenue
Argonne, IL 60439

J. M. Batch
Battelle Memorial Institute
505 King Ave.
Columbus, OH 43201

No. of
Copies

Wayne Carbiener
Battelle Memorial Institute
505 King Ave.
Columbus, OH 43201

J. D. Duguid
Battelle Memorial Institute
505 King Ave.
Columbus, OH 43201

R. E. Heineman
Battelle Memorial Institute
505 King Ave.
Columbus, OH 43201

J. Kircher
Battelle Memorial Institute
505 King Ave.
Columbus, OH 43201

Don Moak
Battelle Memorial Institute
505 King Ave.
Columbus, OH 43201

Ken Yates
Battelle Memorial Institute
505 King Ave.
Columbus, OH 43201

Brookhaven National Laboratory
Reference Section
Information Division
Upton, NY 11973

Paul W. Levy
Brookhaven National Laboratory
Upton, NY 11973

M. Steinberg
Brookhaven National Laboratory
Upton, NY 11973

Cumbustion Division
Combustion Engineering, Inc.
Windsor, CT 06095

B. Adams
Corning Glass Works
Technical Staffs Division
Corning, NY 14830

E. Vejvoda, Director
Chemical Operations
Rockwell International
Rocky Flats Plant
P.O. Box 464
Golden, CO 80401

No. of
Copies

J. L. Crandall
E. I. duPont DeNemours and Company
Savannah River Laboratory
Aiken, SC 29801

H. L. Hull
E. I. duPont DeNemours and Company
Savannah River Laboratory
Aiken, SC 29801

R. G. Garvin
E. I. duPont DeNemours and Company
Savannah River Laboratory
Aiken, SC 29801

S. Mirshak
E. I. duPont DeNemours and Company
Savannah River Laboratory
Aiken, SC 29801

D. L. McIntosh
E. I. duPont DeNemours and Company
Savannah River Laboratory
Aiken, SC 29801

J. A. Kelley
E. I. duPont DeNemours and Company
Savannah River Laboratory
Aiken, SC 29801

S. D. Harris, Jr.
E. I. duPont DeNemours and Company
Savannah River Laboratory
Aiken, SC 29801

Robert Maher
E. I. duPont DeNemours and Company
Savannah River Laboratory
Aiken, SC 29801

M. S. Plodinec
E. I. duPont DeNemours and Company
Savannah River Laboratory
Aiken, SC 29801

A. S. Jennings
E. I. duPont DeNemours and Company
Savannah River Laboratory
Aiken, SC 29801

Leon Meyers
E. I. duPont DeNemours and Company
Savannah River Laboratory
Aiken, SC 29801

H. Henning
Electric Power Research Institute
3412 Hillview Avenue
P.O. Box 10412
Palo Alto, CA 94301

No. of
Copies

Environmental Protection Agency
Technology Assessment Division
(AW-559)
Office of Radiation Programs
Washington, DC 20460

R. G. Barnes
General Electric Company
175 Curtner Avenue (M/C 160)
San Jose, CA 95125

L. H. Brooks
Gulf Energy and Environmental Systems
P.O. Box 81608
San Diego, CA 92138

E. S. Goldberg
Savannah River Operations Office
P.O. Box A
Aiken, SC 29801

D. C. Fulmer
Savannah River Operations Office
P.O. Box A
Aiken, SC 29801

3 Los Alamos Scientific Laboratory (DOE)
P.O. Box 1663
Los Alamos, NM 87544

C. J. Kershner
Monsanto Research Corporation Mound
Laboratory
P.O. Box 32
Miamisburg, OH 45342

John Pomeroy
Technical Secretary
National Academy of Sciences
Committee of Radioactive Waste
Management
National Research Council
2101 Constitution Avenue
Washington, DC 20418

S. D. Barrett
New England Power Company
280 Melrose Street
Providence, Rhode Island 02901

2 J. P Duckworth
Plant Manager
Nuclear Fuel Services, Inc.
P.O. Box 124
West Valley, NY 14171

J. G. Cline, General Manager
NYS Energy Research and Development
Authority
230 Park Avenue, Rm 2425
New York, NY 10017

No. of Copies

2 Oak Ridge National Laboratory (DOE)
Central Research Library
Document Reference Section
P.O. Box X
Oak Ridge, TN 37830

E. H. Kobish
Solid State Division
Oak Ridge National Laboratory
Oak Ridge, TN 37830

G. J. McGarthy
Pennsylvania State University
Materials Research Laboratory
University Park, PA 16802

D. R. Anderson
Sandia Laboratories
Albuquerque, NM 87107

J. K. Johnstone
Sandia Laboratories
Albuquerque, NM 87107

W. Weart
Sandia Laboratories
Albuquerque, NM 87107

J. Sivinshi
Sandia Laboratories
Albuquerque, NM 87107

J. O. Blomeke
Union Carbide Corporation (ORNL)
Chemical Technology Division
P.O. Box Y
Oak Ridge, TN 37830

2 D. E. Ferguson
Union Carbide Corporation (ORNL)
Chemical Technology Division
P.O. Box Y
Oak Ridge, TN 37830

H. W. Godbee
Union Carbide Corporation (ORNL)
Chemical Technology Division
P.O. Box Y
Oak Ridge, TN 37830

W. C. McClain
Union Carbide Corporation (ORNL)
Chemical Technology Division
P.O. Box Y
Oak Ridge, TN 37830

R. A. Beall
U. S. Department of Interior Bureau of Mines
Albany Research Center
1450 W. Queen Avenue
Albany, OR 97321

No. of Copies

D. B. Stewart
U. S. Department of Interior
959 National Center
Geological Survey
Reston, Virginia 22092

R. G. Post
College of Engineering
University of Arizona
Tucson, AZ 85721

S. E. Logan
Los Alamos Technical Associates, Inc.
P.O. Box 410
Los Alamos, NM 87544

FOREIGN

2 International Atomic Energy Agency
Kärtner Ring 11
P.O. Box 590
A-1011, Vienna, AUSTRIA

Rene Amavis
EURATOM
Health Physics Division
29, Rue Aldringer
Luxembourg, BELGIUM

G. G. Strathdee
Atomic Energy of Canada, Ltd.
W.N.R.E. Pinawa, Manitoba
ROE 1LO
CANADA

M. Tomlinson
Director of Chemistry and Materials Science Division
Atomic Energy of Canada Ltd.
Whiteshell Nuclear Research Establishment
Pinawa, Manitoba, CANADA

K. D. B. Johnson
Atomic Energy Research Establishment,
Harwell, Didcot,
Berks, ENGLAND

J. A. C. Marples
Atomic Energy Research Establishment
Harwell, Didcot,
Berks, ENGLAND

D. W. Clelland
United Kingdom Atomic Energy Authority
Risley, ENGLAND

No. of
Copies

FOREIGN

P. J. Regnaut
Centre d'Etudes Nucleaires de
Fontenay-aux Roses
Boite Postale 6
92 - Fontenay-aux Roses
FRANCE

Y. J. Sousselier
Center d'Etudes Nucleaires
de Fontenoy-aux Roses
Boite Postale 6
92 - Fontenay-aux Roses
FRANCE

Bundesministerium für Forschung und
Technologie
Stressemannstrasse 2
5300 Bonn
WEST GERMANY

Center for Atomic Energy
Documentation (ZAED)
Attn: Dr. Mrs. Bell
P. O. Box 3640
7500 Karlsruhe
WEST GERMANY

Hans W. Levi
Hahn-Meitner Institut
1 Berlin 39
Glienickerstr. 100
WEST GERMANY

E. R. Merz
Institut für Chemische
Technologie
Kernforschungsanloge Julich
GmbH
D517 Julich
Postfach 365
Federal Republic
WEST GERMANY

R. Bonniand
Center de Marcoule
B.P. 170
30200 Baguols-Sur-Ceze
FRANCE

C. Sombret
Centre de Marcoule
B.P. 170
30200 Baguols-Sur-Ceze
FRANCE

F. Laude
Centre de Marcoule
B.P. 170
30200 Baguols-Sur-Ceze
FRANCE

No. of
Copies

FOREIGN

H. Krause
Kernforschungszentrum Karlsruhe GmbH
(KfK)
Postfach 3640
D7500 Karlsruhe
WEST GERMANY

R. V. Amalraj
C.W.M.F. Project
P.O. Kalpakkam
Chingleput Dist.
Tamil Nadu, INDIA

N. S. Sunder Rajan
Bhabha Atomic Research Centre
Goverment of India
Hall No. 5
Trombay
Bombay 8S
INDIA

Dr. Piero Risoluti,
AGIP NUCLEARE
c/o COMB Casaccia
C.P. 2400
Rome
ITALY

F. Gera
CHEN
CSN Casaccia L.I.S.
C.P. 2400, 00100
Rome
ITALY

S. Tashiro
Japan Atomic Energy Research Institute
Environmental Safety Research
Laboratory
1-1-13, Shibashi
Minatopku, Tokyo
JAPAN

ONSITE

3 DOE Richland Operations Office

H. E. Ransom
M. W. Shupe
M. J. Zamorski

11 Rockwell Hanford Operations

H. Badad
R. A. Deju
R. J. Gimera
J. D. Kaser
E. J. Kosiancic
M. J. Kupfer
C. M. Manry

No. of Copies

ONSITE

J. H. Roecker
W. W. Schultz
D. D. Wodrich
File copy

3 Exxon Nuclear Company

S. J. Beard

Joint Center for Graduate Study

J. Cooper

2 United Nuclear Industries, Inc.

T. E. Dabrowski
A. E. Engler

Westinghouse Hanford Company

A. G. Blasewitz

72 Pacific Northwest Laboratory

T. W. Ambrose
W. J. Bjorklund
H. T. Blair
W. F. Bonner
D. J. Bradley
A. Brandstetter
R. L. Bunnell
H. C. Burkholder
N. E. Carter
C. C. Chapman
L. A. Chick
T. D. Chikalla
M. O. Cloninger
J. W. Finnigan
A. A. Garrett
W. J. Gray
M. S. Hanson
J. C. Hartl
M. H. Henry (3)
O. F. Hill
J. H. Jarrett
Y. B. Katayama
W. S. Kelly
R. S. Kemper
D. E. Knowlton
D. K. Kreid
W. L. Kuhn
D. E. Larson
J. M. Lukacs
R. P. Marshall
J. L. McElroy (10)
J. S. McPherson

No. of Copies

ONSITE

G. B. Mellinger
J. E. Mendel
R. E. Nightingale
D. E. Olesen
C. R. Palmer
A. M. Platt
D. L. Prezbindowski (2)
F. P. Roberts
W. A. Ross
J. M. Rusin
D. H. Siemens
S. C. Slate
R. T. Treat
R. P. Turcotte (2)
H. H. Van Tuyl
J. W. Voss
J. W. Wald/W. E. Weber
J. H. Westsik, Jr.
L. D. Williams
W. K. Winegardner
Technical Information (5)
Publishing Coordination (2)